



Biofilm development of *Bacillus siamensis* ATKU1 on pristine short chain low-density polyethylene: A case study on microbe-microplastics interaction

Abhrajyoti Tarafdar^{a,1}, Jae-Ung Lee^{b,2}, Ji-Eun Jeong^c, Hanbyul Lee^{a,3}, Yerin Jung^{a,4}, Han Bin Oh^{b,5}, Han Young Woo^{c,6}, Jung-Hwan Kwon^{a,*,7}

^a Division of Environmental Science and Ecological Engineering, Korea University, 145 Anam-ro, Seongbuk-gu, Seoul 02841, South Korea

^b Department of Chemistry, Sogang University, 35 Baekbeom-ro, Mapo-gu, Seoul 04107, South Korea

^c Department of Chemistry, Research Institute for Natural Sciences, Korea University, 145 Anam-ro, Seongbuk-gu, Seoul 02841, South Korea

ARTICLE INFO

Keywords:

LDPE
Biofilm
Microplastics
Biodegradation
Van Krevelen

ABSTRACT

A low-density polyethylene (LDPE) degrading bacterial strain (ATKU1) was isolated (99.86% similar with *Bacillus siamensis* KCTC 13613^T) from a plastic dumping site to study interactions between microplastics (< 5 mm) and microorganisms. The strain was found (by scanning electron microscopy) to form biofilm on the microplastic surface after its interaction with LDPE (avg. $M_w \sim 4,000$ Da and avg. $M_n \sim 1,700$ Da) as a sole carbon source. Atomic force microscopy (AFM) showed the biofilm's 3-D developmental patterns and significantly increased Young's modulus of the LDPE surface after microbial treatment. Most of the viable bacteria attached to biofilms rather than media, which suggested their ability to utilize LDPE. Absorption bands of carbonyl, alkenyl, acyl, ester, primary-secondary alcohol, alkene groups and nitric oxides were found on the treated LDPE particles using Fourier-transform infrared spectroscopy. Fourier transform-ion cyclotron resonance mass spectrometry of the media indicated compositional shifts of the compounds after treatment (i.e., increase in the degree of unsaturation and increment in oxygen-to-carbon ratio) and presence of unsaturated hydrocarbons, polyketides, terpenoids, aliphatic/peptides, dicarboxylic acids, lipid-like compounds were hinted. The plastic degrading abilities of *Bacillus siamensis* ATKU1 suggest its probable application for large scale plastic bioremediation facility.

1. Introduction

Worldwide plastic production has dramatically increased since the industrial scale production of synthetic polymeric materials began in the 1940s and 1950s, arriving at 359 million metric tons in 2018 (Garside, 2019). Thirteen million tons of plastics are introduced to the sea and coastal areas each year, representing a genuine and developing danger to marine biodiversity and probably human well-being (United Nations, 2018). Plastic debris can directly affect the fauna (especially marine

birds, reptiles, and mammals), resulting in choking hazards by ingestion, injury, and death due to snaring (Lusher et al., 2018; Stelfox et al., 2016). During its habitation in the terrestrial and aquatic environments, huge plastic garbage becomes fragile and experiences fracture due to weathering processes (i.e., UV, mechanical stress, varying temperatures, salinity, oxidation, etc.), producing microplastics (size < 5 mm). The enormous load of plastic waste may have adverse effects on fish (Wang and Yu, 2020), birds (Basto et al., 2019), and other top consumers (Campani et al., 2013; Hernandez-Gonzalez et al., 2018;

* Corresponding author.

E-mail addresses: abhra@outlook.com, abhra@korea.ac.kr (A. Tarafdar), tnlatnla@sogang.ac.kr (J.-U. Lee), jieunj@korea.ac.kr (J.-E. Jeong), hblee95@korea.ac.kr (H. Lee), qtwree@korea.ac.kr (Y. Jung), hanbinoh@sogang.ac.kr (H.B. Oh), hywoo@korea.ac.kr (H.Y. Woo), junghwankwon@korea.ac.kr (J.-H. Kwon).

¹ 0000-0003-0020-5279

² 0000-0002-6699-2335

³ 0000-0002-7634-9618

⁴ 0000-0003-2276-9585

⁵ 0000-0001-7919-0393

⁶ 0000-0001-5650-7482

⁷ 0000-0002-6341-7562

<https://doi.org/10.1016/j.jhazmat.2020.124516>

Received 10 August 2020; Received in revised form 21 October 2020; Accepted 5 November 2020

Available online 16 November 2020

0304-3894/© 2020 Elsevier B.V. All rights reserved.

Mathieu-Denoncourt et al., 2015) in the environment. On the contrary, microplastics are more likely to be taken in by lower trophic level microorganisms (Botterell et al., 2019). However, a very small number of studies has been conducted on the interactions between microplastics and their probable first-hand consumers with a particular focus on the effects of microplastics in these microorganisms.

In nature, microscopic organisms often exist in immobile networks known as biofilms. Biofilms are phylogenetically and practically different groups of bacteria, algae, protozoans, and fungi mostly called microbial gathering, biofouling network, or periphyton. These microorganisms live in spatial closeness with one another on any surface generally submerged in extracellular polymeric substances (EPS). Biofilm is a solid and dynamic structure that gives an expansive scope of benefits to its individuals, including attachment or adhesion abilities, nutrient aggregation, metabolite interexchange platform (leading to a better use of transformed products), cellular communication, protection, and resistance to chemical and ecological stress conditions (Dos Santos et al., 2018). Studies also suggest that corrosion by bacterial biofilms is better than that by planktonic microscopic organisms (Zettler et al., 2013). Primary attachment of microscopic organisms to the exterior of plastics is followed by the colonization of the uncovered plastic surface. Studies have shown that commencement of biofilms upgrades carbon usage from non-dissolvable substrates like polystyrene and polyethylene (Chauhan et al., 2018).

To understand the interaction between microplastics and potential plastic degrader microbes (attachment process, development of biofilm, activity of the biofilm in the means of carbon usage, cell viability etc.), it is important to study the biofilms on microplastic particles. A small number of publications have been dedicated to the microbial utilization of aquatic plastic wastes, including the effect of plastic on aquatic microbial life guarantees and, conversely, the role of microbial films in plastic degradation. There are a handful of studies on plastisphere (Baptista Neto et al., 2019; Jacquin et al., 2019; Jiang et al., 2018; Kirstein et al., 2018; Zettler et al., 2013) and biofilm formations on microplastics (Chauhan et al., 2018; Miao et al., 2019; Michels et al., 2018; Ogonowski et al., 2018; Parrish and Fahrenfeld, 2019; Pinto et al., 2019), but they lack enough details on morphology of developmental stages and the effects of the formation on microplastic itself.

This study aims to highlight the interaction between aquatic microplastic (taking low-density polyethylene [LDPE] as a model microplastic) and a plastic degrading bacterial strain, *Bacillus siamensis* ATKU1. The morphology of the developmental phases of the biofilm was investigated using scanning electron microscopy (SEM), atomic force microscopy (AFM), and confocal laser scanning microscopy (CLSM). The changes in LDPE microplastic functional groups, incubated with *B. siamensis* ATKU1, were analyzed using Fourier-transform infrared (FTIR) spectroscopy. The metabolites in the solution were also identified using Fourier transform-ion cyclotron resonance (FT-ICR) mass spectrometry.

2. Materials and methods

2.1. Materials

LDPE without catalysts or additives was obtained from Sigma-Aldrich (St. Louis, MO, USA) (average $M_w \sim 4,000$ Da and average $M_n \sim 1,700$ Da by gel permeation chromatography according to the supplier). The physical and chemical properties of the product are provided in Table S1 (Supplementary Material). Microscopic analysis revealed that the particle size of the LDPE is $446.69 \pm 182.14 \mu\text{m}$ (Fig. S1, Supplementary Material). The chemical composition of the product was further characterized using FTIR Cary 630 (Agilent, Santa Clara, California, USA). LDPE was chosen as the model polymer because of its significance both as the most broadly produced polymer, representing 17.3–21% of the worldwide manufactured product, and as a

broadly reported segment of marine plastic garbage (Erni-Cassola et al., 2019; Harrison et al., 2014; Plastics Europe & EPRO, 2016). Another reason for selecting low average-molecular-weight polyethylene was to shorten the experimental time for degradation. The mineral salt medium used for microbial enrichment and biofilm developmental study was Bushnell-Haas broth (HiMedia, Mumbai, Maharashtra, India) composed of (L^{-1} deionized water) K_2HPO_4 , 1 g; KH_2PO_4 , 1 g; NH_4NO_3 , 1 g; CaCl_2 , 0.02 g; MgSO_4 , 0.20 g; FeCl_3 , 0.05 g, and adjusted to pH 7 with NaOH (Tarafdar et al., 2017). The growth medium was Luria Bertani (LB) broth procured from Sigma-Aldrich. All organic solvents (acetone, *n*-hexane, acetonitrile, etc.) used for sample processing and analysis were of HPLC grade (J.T. Baker, Center Valley, PA, USA and Daejung, Siheung, Republic of Korea). Milli-Q water was utilized to perform the diagnostic system.

2.2. Enrichment and isolation of polyethylene-degrading bacteria

The polyethylene-degrading bacteria of interest were isolated by cultivating them in a medium where LDPE was present as the sole carbon source. The mineral salts medium was Bushnell-Haas broth. The medium was sterilized (autoclaved) to eliminate contaminating microbes. LDPE powder (4 g L^{-1}) was transferred to a 1 L Erlenmeyer flask containing 500 mL of carbon-free-medium to prepare the desired enrichment medium. LDPE (floating on media) powder in the water-based medium results in relatively high bacterial accessibility of the only carbon source due to continuous shaking. Ten grams of drainage-side soil sample was collected from a plastic waste dumping site ($22^\circ 28' 1'' \text{N } 88^\circ 22' 21'' \text{E}$) near Kolkata, India using a stainless auger, up to a depth of 10 cm from surface. The sample was transferred to a glass vial to preserve in the dark at 4°C . TOC (%) of the collected soil was 1.62 according to Walkley-Black method, it was classified as loamy sand according to USDA method (Fig. S2, Supplementary Material), and the particle size of the collected soil was $703.90 \pm 251.21 \mu\text{m}$ (Fig. S3, Supplementary Material). The soil was weighed and transferred to 100 mL brine (0.85% NaCl) solution. An aliquot of 5 mL supernatant solution was transferred to the freshly prepared media (containing 4 g L^{-1} LDPE). The Erlenmeyer flask was shaken at 120 rpm and 32°C in a shaking incubator (Wisecube WIS-20, witeg Labortechnik GmbH, Wertheim, Germany). After 45 days of incubation, an aliquot of 5 mL enriched culture was transferred to another 1 L Erlenmeyer flask containing 500 mL fresh Bushnell-Haas broth with 4 g L^{-1} polyethylene for 45 days. This step was repeated three times to attain bacterial strains of interest that can use LDPE as a carbon source. After the end of enrichment, bacterial strains in each consortium were isolated by spreading the 10-fold serial diluted consortium on an LB agar plate. Clear zones of separated bacterial colonies were observed in an overnight. Isolated single colonies were again transferred to the enrichment media (supplemented with LDPE 4 g L^{-1} as the only carbon source) to select the strain with the highest growth rate (by measuring turbidity of the liquid enrichment media at 604 nm). The colony with the highest growth rate was selected from the enrichment culture, further purified by repetitive streaking on LB agar plates, and stored in a final enrichment medium containing LDPE as the sole carbon source.

2.3. Bacterial characterization

The genomic DNA of strain ATKU1 was extracted and purified in accordance with Yoo et al. (2019). Polymerase chain reaction (PCR) was used to amplify the 16S rRNA gene with the universal primers 27F (5'-AGAGTTTGATCCTGGCTCAG-3') and 1492R (5'-TACGGYTACCTTGTACGACTT-3'). PCR was performed with a primary heating step for 3 min at 95°C , 25 cycles of denaturation for 45 s at 94°C , annealing for 45 s at 55°C , and extension for 90 s at 72°C , and a final extension step for 5 min at 72°C . The length of the amplified fragment was assessed using agarose gel electrophoresis and gel-purification with the single band of the result. MacroGen Inc. (Seoul, Republic of Korea) sequenced

the gel-purified fragment. An almost complete 16S rRNA gene sequence (1,455 bp) was determined in this study and was compared to the corresponding sequence from other bacterial species using the EzBioCloud database (Yoon et al., 2017) and the GenBank database using the Basic Local Alignment Search Tool (BLAST) from NCBI (<https://www.ncbi.nlm.nih.gov>).

The phylogenetic analyses of the isolated strain were performed using Mega X. The evolutionary history was computed using the neighbor-joining method. The evolutionary distances were inferred using the Tamura 3-parameter method. The neighbor-joining topology was evaluated using bootstrap analysis with 1,000 replications. Phylogenetic analysis showed that the strain ATKU1 (GenBank accession no. MT454062) possesses high similarity with *Bacillus siamensis* KCTC 13613^T (99.86%) (Fig. S4, Supplementary Material). The strain ATKU1 (Fig. S5, Supplementary Material) belongs to the genus *Bacillus*; clustered with *B. siamensis* KCTC 13613^T, *B. velezensis* CR-502^T, and *B. amyloliquefaciens* DSM 7^T. The isolated strain has been successfully deposited into the general collection of microorganism of the Korean Collection for Type Cultures (KCTC) and accession number of strain ATKU1 is KCTC 43269.

2.4. Biodegradation assay

Successful LDPE biodegradation was characterized using new peak generation in the FTIR spectrum of the biologically treated LDPE, molecular weight shift, and the formation of soluble transformation products in the aqueous mineral salt media (Bushnell-Haas broth). Successful carbon utilization is also supported by the cell viability assay.

The biodegradation assay (batch process) was performed for 45 days in a 1 L conical flask containing 500 mL fresh Bushnell-Haas broth containing 4 g L⁻¹ of LDPE (120 rpm and at 32 °C). The batch procedure was inoculated with 1 mL of bacterial suspension from the final enrichment media (centrifuged, supernatant discarded, pellet resuspended in Milli-Q water, and washed three times in phosphate-buffered saline). The entire degradation experiment was intentionally conducted in the dark to remove the effect of LDPE photodegradation and to solely concentrate on transformed products of microbe-microplastic interaction. The assay was conducted in triplicate along with a sterile control (i. e., LDPE incubated in the media and shaken for 45 days without bacteria). After a 45-day degradation period (LDPE removal 4.71 ± 0.16%, Data S1, Supplementary Material), the remaining LDPE particles were filtered out using a glass microfiber filter (pore size of 1.5 µm, Whatman, UK). The filtrate was centrifuged at 10,000 rpm for 10 min to remove suspended bacterial cells, and the supernatant passed through a solid-phase extraction (SPE) cartridge (Oasis HLB, Waters, Milford, MA, USA). The entrapped transformation products in the SPE cartridge were eluted with 6 mL acetonitrile. The acetonitrile extract was further filtered through a 0.45 µm polyvinylidene fluoride (PVDF) syringe filter (Agilent Technologies) to eliminate any impurity before mass spectrometry.

2.5. Microscopic analysis

Primary visualization of the developed biofilm over LDPE particles was conducted using an Olympus SZ61 binocular microscope mounted with an Olympus DP20 microscopic camera (Olympus, Shinjuku, Japan). Biologically treated and air-dried (in laminar flow cabinet) LDPE particles were directly visualized along with the pristine LDPE particles (× 10 magnification).

Morphology of the evolved biofilms over LDPE was inspected using a scanning electron microscope (SEM) (SU-70, Hitachi, Tokyo, Japan). Minuscule slides of the biofilm-LDPE assemblage were made by immobilizing them with 2.50% glutaraldehyde in phosphate buffer (pH 7.2). Next, serial dehydration with gradually increasing ethanol volumes (10 min incubation duration each) was performed using 30%, 50%, 70%, 80%, 90%, and 100% ethanol solutions. Next, the glass slides of the

samples were fixed in a specimen holder of the high-resolution SEM and analyzed using an in-lens detector. The samples underwent a gold coating in deep vacuum for better perceivability. The slides were observed at extra high-tension accelerating voltage (EHT) 2.00–5.00 kV, × 3.00–3.50 K magnification, and a working distance of 10–12 mm.

AFM imaging was performed using an XE-100 (Park Systems, Seoul, Republic of Korea) microscope with an Al coated PPP-NCHR cantilever (tip radius < 10 nm) in non-contact operating mode. The scan rate was 0.5 Hz. Topography images were initially handled by XEI data processing and analysis software 4.3.4 (Park Systems). A 256-pixel count was used to acquire images of the biofilm growth on LDPE surfaces. The scan size for the biofilm and raw LDPE surface was selected as 10 µm based on resolution and magnification. The LDPE from the batch process, which underwent biological treatment, was collected using filtration (glass microfiber filter, pore size of 1.5 µm, Whatman) and washed with phosphate-buffered saline (pH 7.2) at 150 rpm for 1 min to remove the loosely-bound cells from the biofilm. Biofilm-LDPE aggregates were air-dried on a glass slide and immobilized using a double-sided carbon tape. The biofilm-on-LDPE surface (examined at regular intervals of ten days after the lag phase) was scanned at three randomly chosen areas and plots were made to deliver a three-dimensional portrayal of the surface. The height images were examined using Gwyddion 2.53 (Czech Metrology Institute, Jihlava, Czech Republic) software. Mean roughness (Sa), root-mean-square roughness (Sq), maximum peak height (Sp), maximum pit depth (Sv), skewness and excess kurtosis of the evolved biofilm were estimated. The Sa is the arithmetic average deviation of the height esteems from the mean surface. Comparably, the Sq is the root-mean-square average of standard height deviation taken from the mean plane (Huang et al., 2015). Skewness and kurtosis of the biofilm characterize the existence of valleys and/or hills amid the image data plane. Table S2 (Supplementary Material) provides the insights of the AFM parameters.

2.6. Cell viability

The biofilms on the LDPE surface were stained using the Live/Dead BacLight Bacterial Viability Kit L13152 (Invitrogen, Carlsbad, CA, USA) according to the manufacturer's suggestions. The kit contains the SYTO9 green-fluorescent nucleic acid stain and the red-fluorescent nucleic acid stain, propidium iodide. These stains contrast both in their spectral attributes and in their capacity to infiltrate healthy bacterial cells. LDPE particles without biofilm were also stained to exclude any false positive signals. The excitation/emission maxima for the stains are 480/500 nm for SYTO 9 and 490/635 nm for propidium iodide.

Post-treated LDPE particles with developed biofilms were filtered out of the media (after 15th, 30th, and 45th day of treatment) and washed out with 0.85% NaCl solution to remove loosely bound microbes. The stain mixture was applied directly on biofilm covered LDPE in the culture dish (50-mm glass-bottom). Media (30 × 2 mL) was centrifuged (CF-10, Daihan Scientific, Wonju, Republic of Korea) at 10,000 rpm for unattached bacteria in aqueous medium. The supernatant was discarded, and the sedimented pellet was resuspended in 20 mL of 0.85% NaCl. The samples were incubated for 1 h and centrifuged again to generate a pellet while discarding the supernatant. This pellet was resuspended into 5 mL of stain mix and transferred into culture dishes. All the samples were incubated at room temperature (~25 °C) in the dark for 15 min and subjected to confocal laser scanning microscopy (CLSM). A Zeiss LSM 700 CLSM was used with Zeiss Zen 2012 software (Carl Zeiss, Oberkochen, Germany). A Plan-Apochromat objective was used to observe and digitally capture images (1,024 × 1,024 pixel, 24 bit) at a × 20 magnification (numerical aperture 0.8, free working distance 0.55 mm, cover glass thickness 0.17 mm, thread type M27 × 0.75, field of view 25 mm). ImageJ (National Institutes of Health, Bethesda, Maryland, U.S.) software (version: 1.52a) with Color Pixel Counter plugin was used to calculate the green and red pixel count of each image, which indicated the live to dead cell ratio.

2.7. FTIR and mass spectrometry

Point-by-point data regarding bio-catalytically initiated changes in substance structures of control plastics (incubated in the media and shaken for 45 days without bacteria) and their conceivable transformation products were obtained using FTIR spectroscopy (Cary 630, Agilent USA; Germanium ATR accessory). This was performed on LDPE powder incubated with and without biological treatment using attenuated total reflectance (ATR) mode. The LDPE powder samples obtained after the biological treatment were repeatedly (Milli-Q) washed to remove attached bacterial cells, dried under vacuum conditions, and put away in vacuum desiccators. Triplicate scans were performed without any significant deviations among the results. Careful background scanning was also conducted to limit the noise in the spectrum. IR spectra of all samples were recorded in the range 400–4,000 cm^{-1} .

Ultrahigh resolution mass spectra were acquired using a 15T FT-ICR mass spectrometer equipped with an electrospray ionization (ESI) source (solariXTM system, Bruker Daltonics, Billerica, MA, USA). The instrument was calibrated using a solution of sodium trifluoroacetate cluster before analysis. The ESI mass spectra were obtained in both positive and negative mode for the metabolite samples and control (i.e., LDPE incubated in sterile media) samples. A 200 μL aliquot of each sample was vortex-mixed with 100 μL of arginine solution (0.5 g L^{-1} in water) for internal calibration. The analytes were directly infused into the mass spectrometer at a flow rate of 120 $\mu\text{L h}^{-1}$ with a syringe pump, and 100 scans were collected for each sample over the mass range of m/z 160–1150. The accumulation time was adjusted at 0.25 s for all experiments. The other parameters were as follows: spray voltages: + 3.0 kV for positive ion mode and – 3.5 kV for negative ion mode; drying gas temperature, 210 $^{\circ}\text{C}$; drying gas flow rate, 4.0 L min^{-1} .

The peak-finding and internal calibration were performed using data analysis software 4.1 (Bruker Daltonics). Peak lists were generated from the raw data using the criterion of signal-to-noise ratio ≥ 10 . Internal calibration was conducted using a series of arginine cluster (m/z range 175.11895–871.56565) peaks, and the resulting standard deviations were less than 0.2 ppm. The acquired peak lists were data-processed using an in-house MATLAB (MathWorks, Inc., Natick, MA, USA) code and database (Begum et al., 2019). The database was constructed to

contain all possible chemical composition satisfying the following criteria: $0.3 < \text{H/C} < 3.0$, $\text{O/C} < 1.0$, $\text{N/C} < 1.0$, $\text{H} \leq 2\text{C} + \text{N} + 2$. Identification was made with the criterion of error ≤ 1.0 ppm in the range m/z 200–800. New peak lists were made from the peak lists of the control media and treated media samples by selecting the theoretical m/z values, which were found only in the (biologically) treated media sample. These peak lists were visualized using van Krevelen diagrams (Kim et al., 2003; Van Krevelen, 1950) in Microsoft™ Excel.

3. Results and discussion

3.1. Biofilm formation on LDPE

It is suggested that biofilms improve carbon utilization from non-dissolvable substrates like LDPE. Intracellular and/or extracellular depolymerases are generally the key enzymes for the degradation of polymers. Non-hydrolysable polymers like LDPE can undergo a breaking down of C-H chains via strong oxidative enzymes; thereafter can be hydrolyzed into monomers, dimers, or oligomers by the bacterial extracellular depolymerases and penetrate through the cellular membrane of the microbes to be used as a carbon source (Chauhan et al., 2018).

Light microscopic images of the pristine and treated LDPE particles showed the traces of developed biofilm on the LDPE surface (Figs. 1a–b, and S6 of Supplementary Material). Digging deeper, the high-resolution scanning electron microscopic image shows the biofilm on the LDPE surface. The pristine sample (Fig. 1c) has an appearance of relatively plain surface with no pits, breaks, or any particles appended superficially, but we noticed a typical texture on pristine LDPE surface. The control (i.e., LDPE incubated in sterile media) shows similar characteristics (Fig. S7, Supplementary Material). On the 15th day of the treatment (Fig. 1d), organisms were found attached on the surface, forming a microbial film with a solid adherence ability and the potential to use LDPE as a carbon source. Surprisingly, 15-day treated LDPE surface looked smoother, and typical textures from pristine LDPE surface disappeared, which can be an effect of the extracellular depolymerase activity of the biofilm (Fig. S8, Supplementary Material). A single bacterium from the biofilm appeared to be approximately 1 μm in length

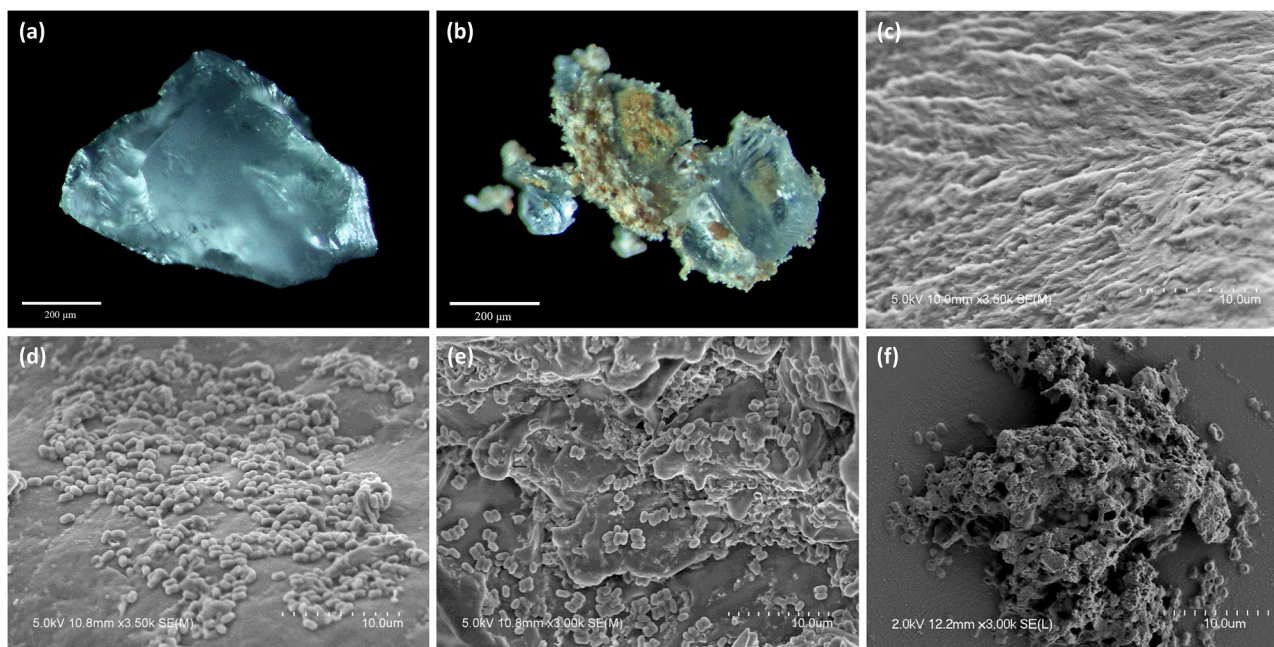


Fig. 1. (a–b) Light microscopic images ($\times 10$ magnification) of a pristine and treated LDPE particle with biofilms developed on the treated particle surface, (c) SEM image of pristine LDPE surface, (d) newly formed biofilm onto the surface of LDPE (15th day in batch culture), (e) 30-day treated sample with some extracellular polymeric substance deposition, (f) a tiny and heavily corroded single LDPE particle at the 45th day of the batch treatment.

and 0.5 μm in breadth. A 30-day treated sample (Fig. 1e) showed the developed biofilm with EPS deposition throughout the biofilm. Deposited EPS are likely water-insoluble oligomers generated by the extracellular depolymerase activity of bacteria or adhered water-insoluble metabolites. Subsequent FTIR analysis revealed the presence of a carbonyl group on the treated LDPE surface. Carbonyl compounds with long hydrocarbon tails with low water solubility would explain this deposition. Clearer LDPE corrosion/degradation could be observed at the 45th day of treatment (Fig. 1f). The tiny single LDPE particle was entirely covered with biofilm and metabolic depositions, cavities and craters were noticeable.

3.2. Morphology of biofilm formation on LDPE

Adherence of bacteria on LDPE surface and evolution and the morphology of the biofilm was observed using AFM micrographs. Bacterial cells from the batch treatment media in general were attracted toward the LDPE surface and structure colonies or states superficially. The steady improvement of the biofilm was inspected at regular intervals in the interim (Fig. 2a–e).

According to our procured surface insights information, Sq increased with time until the 25th day of the treatment, before decreasing. Bacterial cells increased the Sq of LDPE surface while getting attached to develop biofilm. This agrees with earlier studies (Chatterjee et al., 2014; Tarafdar et al., 2018) for biofilm development on different material surfaces. The Sq of the pristine LDPE surface (Fig. 2a) (34.99 ± 5.81 nm) suddenly increased after attachment of bacteria on the 15th day (Fig. 2b) of the treatment (180.67 ± 7.65 nm) (the SEM image of 15th day of study is relatable). This trend continued until the 25th day (Fig. 2c) (265.16 ± 28.07 nm) while the bacterial attachment and biofilm development continued. On the 35th day of treatment (Fig. 2d), a slight decrease in Sq (148.51 ± 9.60 nm) was observed, i.e., the LDPE-biofilm aggregate became smoother. The conceivable explanation behind the decrease in roughness at the 35th day might be metabolic discharges from the biofilm and microorganisms were mostly “embedded in EPS” (Rummel et al., 2017). This decrease continued until

the 45th day of treatment (Fig. 2e) (81.99 ± 7.92 nm).

A visual examination on the AFM micrographs revealed clear bacterial adherence on the 15th day and 25th days until the deposited EPS roughly covered bacteria in the biofilm, leaving partial visibility of bacteria on the 35th day scan. On the last day of treatment, the deposited EPS formed a layer on the surface completely sinking the biofilm, making the surface even smoother and leaving the bacteria entirely covered. This typical interactive growth pattern is very special and must be common for polymeric substances like LDPE, since water-insoluble polymeric metabolites tend to deposit on the surface of the biofilm-LDPE aggregate. Other surface properties (Sa, Sp, and Sv) of the biofilm-LDPE aggregate surface followed the same trend (Fig. S9, Supplementary Material).

Negative estimation of skewness showed preeminence of valleys and craters on the image plane, while higher estimations of skewness demonstrated hill predominance (Chatterjee et al., 2014). For symmetric unimodal distributions, positive kurtosis demonstrates presence of peaks/ridges relative to the normal distribution, while negative kurtosis indicates flatness. In short, skewness indicates peaks vs. valleys, and kurtosis shows the sharpness density of the peaks (Liu et al., 2015). Pictorial depiction of surface topographies for skewness and kurtosis maps are presented in Fig. S10, Supplementary Material. The pristine LDPE has a slightly negative skewness (-0.06 ± 0.01) along with a negative kurtosis value (-0.10 ± 0.03), which indicates that pristine LDPE has shallow valleys. The skewness largely increased (0.92 ± 0.04) after the 15th day of treatment mainly because bacterial attachment on LDPE surface formed hill patterns. The positive kurtosis value (0.08 ± 0.00) also signified the appearance of the domes. On the 25th day of treatment, slightly negative skewness (-0.07 ± 0.00) with unchanged kurtosis (0.08 ± 0.01) values signified that the biofilm began to spread on the LDPE surface forming large flat domains. This growth pattern might be supported by a previous study where they were called “multicellular mushroom-like structures” (Sivan et al., 2006). The 35th day sample showed a large negative skewness value (-0.62 ± 0.02) and a near-zero-value of kurtosis, indicating the formation of craters/pits in the plateau-like biofilm surface. The final sample from the 45th day

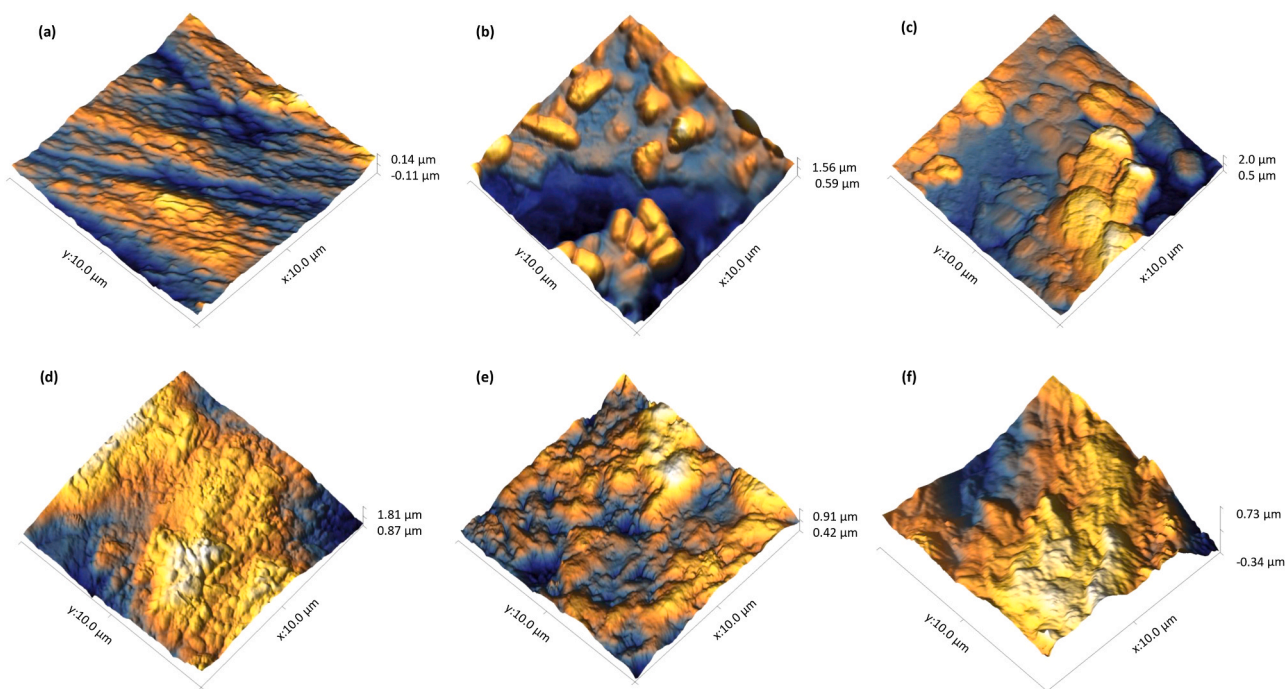


Fig. 2. AFM height images and topography of biofilm formation by strain ATKU1 on LDPE surface. The step-by-step development of biofilm was observed, (a) pristine LDPE, (b) 15th day of treatment, (c) 25th day of treatment, (d) 35th day of treatment, and (e) 45th day of treatment. (f) AFM micrograph of treated LDPE surface with washed out biofilm.

generated a positive skewness (0.05 ± 0.01) along with a relatively high kurtosis (0.20 ± 0.04), indicating that metabolite depositions are filling up the craters and eventually forming small peaks and ridges.

3.3. Changes in LDPE surface

The LDPE particles were washed with 2% (w/v) sodium dodecyl sulfate for 4 h, sterilized with 70% (v/v) ethanol for 4 h, and rinsed with Milli-Q water to remove the attached microbial cells and residual metabolites to examine corrosion (Peixoto et al., 2017; Sivan et al., 2006).

The bacteria-free biodegraded LDPE surface (Fig. 2f) differed greatly from the pristine surface (Fig. 2a). The corroded surface became approximately five times rougher than the pristine surface (Sq of the pristine LDPE: 34.99 ± 5.81 , whereas Sq of the treated LDPE: 173.69 ± 11.52). Changes in skewness and kurtosis values were also clearly noticeable. As we previously observed, the pristine LDPE surface provides a slightly negative skewness value (-0.06 ± 0.01) accompanied by a negative kurtosis value (-0.10 ± 0.03), which indicates that pristine LDPE has shallow valleys. In the case of the 45-day treated LDPE surface, we noticed a large negative skewness value (-0.51 ± 0.08) along with a less negative (compared to the pristine surface) kurtosis value (-0.04 ± 0.01). This change in skewness and kurtosis data indicates development of large pits and craters on the treated LDPE surface.

Changes in the LDPE surface elastic property after the microbial treatment were also observed using the AFM Pinpoint Nanoindentation mode. We used the Sneddon model in XEI data processing and analysis software 5.1.4 (Park Systems) to calculate Young's modulus (definition provided in Data S2, Supplementary Material) of the pristine and treated LDPE surfaces (triplicate study). Significantly increased Young's moduli

(from 223.37 ± 17.96 MPa to 656.51 ± 101.47 MPa) were shown on the LDPE surface in Fig. S11 (Supplementary Material) after treatment. Increments in Young's modulus were previously reported due to the LDPE UV/weathering/ageing process (Al-Salem, 2019, 2015; Tavares et al., 2003), which also signifies increasing brittleness with decreased strain at break (Benítez et al., 2013). Increased crystallization temperature (from 94.5°C for pristine LDPE to 95.8°C for treated LDPE by differential scanning calorimetry, Data S3, Supplementary Material) supports that the increase in brittleness is due to increased crystallinity of residual LDPE.

The low molecular weight fraction of LDPE also reduced significantly because of the biodegradation process (M_w 9,569 Da and M_n 4,242 Da by gel permeation chromatography for residual LDPE after treatment, Data S4, Supplementary Material).

3.4. Cell viability

In our batch culture condition, insoluble LDPE is the only carbon source and hypothetically, alive bacteria should remain in contact to the carbon source in order to survive. Live/dead assay with the LIVE/DEAD BacLight bacterial viability kit helped to understand the viability conditions of the biofilm in our system, and eventually to demonstrate the above-mentioned hypothesis. 15, 30 and 45-day treated LDPE particles were treated with the dyes and subjected to confocal microscopy. 15-day old biofilm (Fig. 3a) showed distinctly attached cells on the LDPE surface, which has 12.55 times more live cells than dead cells according to image color analysis using ImageJ. This denotes a thin healthy freshly developed biofilm, in which bacteria are surviving on the use of LDPE as carbon source. Bacteria taken from liquid media after 15 days of treatment shows this live/dead cells ratio as 0.74 only (Fig. 3d). Noticeably,

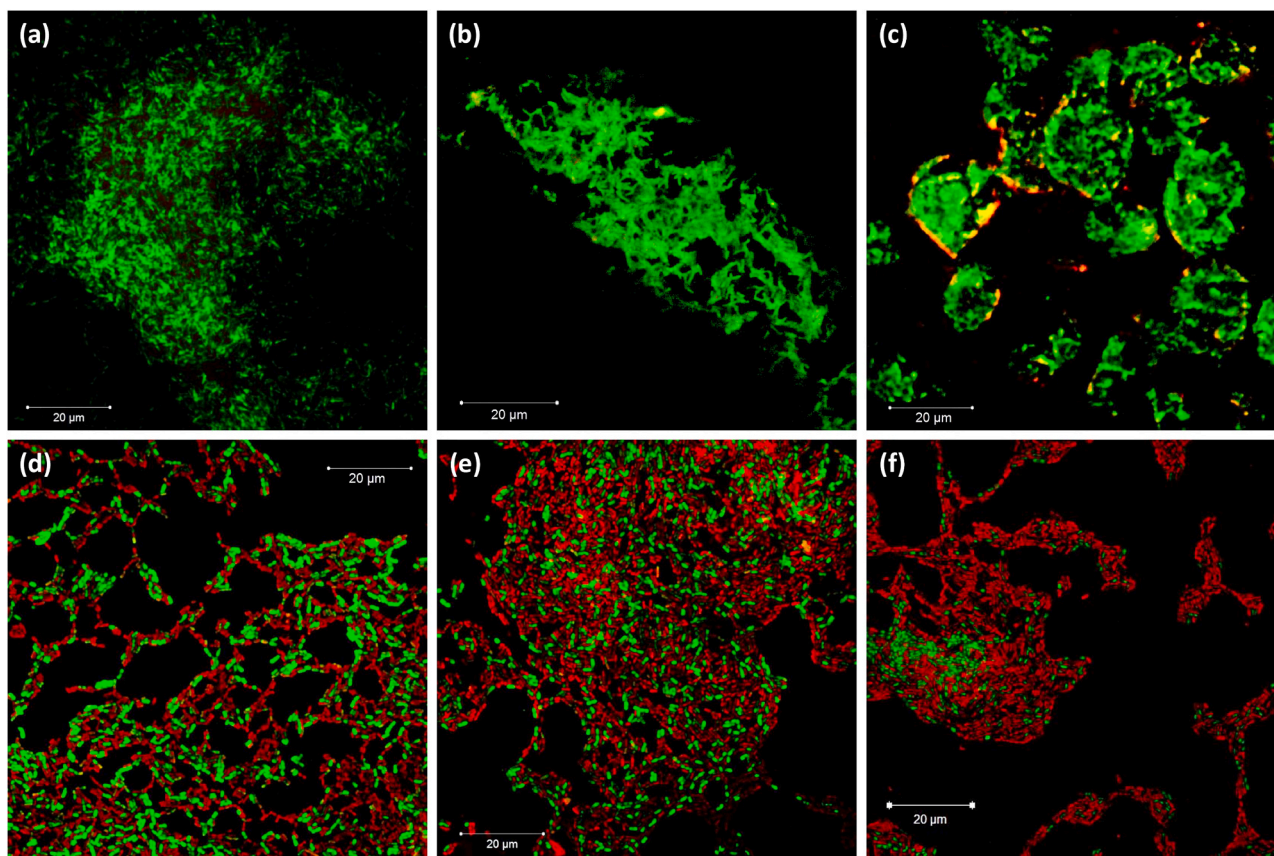


Fig. 3. Cell viability assay. Confocal laser scanning microscopic images of (a–c) biofilms on the LDPE surface and (d–f) cells from the media separated from LDPE particles. Live cells are green and dead cells are red. The images show cell viability after the (a, d) 15th, (b, e) 30th, and (c, f) 45th days of incubation. (For interpretation of the references to colour in this figure legend, the reader is referred to the web version of this article.)

in liquid media there are more dead cells than live cells which withstands our hypothesis that bacteria in biofilm are alive because of direct contact with carbon source.

After 30 days of treatment, the biofilm became thicker and some dead cells overlapped with live cells (yellow color coded) (Fig. 3b). The live/dead cell ratio became relatively lower, but there were still 6.60 times more live cells than dead cells. The corresponding cell count from liquid media had a live/dead cells ratio of only 0.48 (Fig. 3e). A few visible dead cells were found on the LDPE surface on the final treatment day, but there were still 3.11 times more live cells than dead cells (Fig. 3c). EPS retention and/or biofilm thickening would have affected the CLSM image quality causing blurriness with increased time. We noticed that the live/dead cell ratio became as low as 0.24 for the final day in liquid culture medium (Fig. 3f). This indicated that dead cells probably lost their adhesion to LDPE and eventually ended up in the liquid media, detaching from the biofilm. The live/dead cell ratio was only 0.02 in the case of control (i.e., bacteria, in carbon source/LDPE free media) at the end of the study (Fig. S12, Supplementary Material). A negligible number of live cells were found in the media-without-carbon-source, which may be living on reusing the carbon from dead cells. This is the reason we can see cell-clot formations in the control study. The cell viability study shows that the strain ATKU1 can use the polymer (LDPE) as a carbon source.

3.5. FTIR and mass spectrometry: effects of biodegradation

The novel spectroscopic fingerprints of the treated LDPE appeared differently compared to the control (incubated in the media and shaken for 45 days without bacteria) LDPE (Fig. 4a), allowing us to focus on the compound adjustments caused by bacteria. The absorption bands at wavelength 719 and 730 cm^{-1} (rocking deformation), 1,379 cm^{-1} (CH_3 symmetric deformation), 1,463 and 1,472 cm^{-1} (bending deformation), 2,847 and 2,914 cm^{-1} (CH_2 symmetric and asymmetric stretching) are the native bonds present in LDPE (John, 2000; Jung et al., 2018).

Absorption bands at 1,050–1,125 cm^{-1} show a primary and secondary alcohol C–O (alkoxy) stretch. This is accompanied by bands at 3,200–3,400 cm^{-1} , which are assigned to the normal polymeric OH stretch. These two bands signify generation of alcohols via LDPE hydroxylation. The presence of alkane hydroxylase activity by *Bacillus subtilis* was reported earlier (Parthipan et al., 2017) (a phylogenetically neighboring species with similar genome sequence), and the gene for hydroxylase activity was found in another similar strain *Bacillus* sp. GZB (99% identical sequence to *Bacillus siamensis* KCTC13613^T) (Das et al., 2019).

Absorption at 1,163–1,200 cm^{-1} signifies a C–O stretch for ester formation. The presence of ester was previously reported in LDPE biodegradation (Eyheraguibel et al., 2017; Paço et al., 2017; Peixoto et al., 2017), and ester formation due to microbial activity on alkanes was documented (Albertsson et al., 1987). Oxidoreductase enzyme can catalyze ester and keto formation (Harshvardhan and Jha, 2013), and production of this enzyme (laccase) was reported in *B. siamensis* (Gong et al., 2017).

We found a stretching band for the acyl group at absorption of 1,220 cm^{-1} , which is usually a derivative of carboxylic acid (Peixoto et al., 2017). The carboxylic group is a common polyethylene oxidation product (Jacquin et al., 2019). The ester can be hydrolyzed by extracellular esterases, producing carboxylic acid and alcohol end groups (Eyheraguibel et al., 2017). *B. siamensis* has previously tested positive for esterase activity (Sumpavapol et al., 2010).

Nitric oxide synthase (NOS) is a signaling protein that shields Gram-positive strains from anti-infection agents and oxidative stress. NOS enzymatically produces nitric oxide (NO) in *Bacillus subtilis* (bsNOS gene) (Holden et al., 2015). Genes for NOS have also been found in *Bacillus amyloliquefaciens* (nirK gene) (Pinto et al., 2018) and *Bacillus siamensis* (CWD84_18155 gene) (Pan and Ju, 2018). All three species share very similar core genome sequences (Fan et al., 2017).

Fascinatingly, the product of NOS (i.e., NO) is believed to have an important regulatory role in biofilm development (Arora et al., 2015; Hossain et al., 2017). In this scenario, it is postulated that the signal at 1,505–1,569 cm^{-1} can indicate the presence of nitro groups. This signal may also come from residue of bacterial cells which secreted bio-surfactant or proteins to enhance LDPE degradation. A previous study on polyethylene oxidation under a corrosive NO_x atmosphere provides a clue that NO can be responsible for LDPE biodegradation (Oluwoye et al., 2016). Although the partial pressure of NO_x under ambient laboratory condition should be much lower than the condition in Oluwoye et al. (2016); it is worthwhile to investigate free radical reactions of LDPE initiated by NO_x.

The presence of an alkene group is evident because the 960–995 cm^{-1} absorption band for alkene C=C bending and 1,635–1,650 cm^{-1} absorption band for alkenyl C=C stretch were prominently visible. Previous studies reported clear presence of an alkene group for LDPE biodegradation (Mukherjee et al., 2018; Ojha et al., 2017; Peixoto et al., 2017; Sathish et al., 2019). The pathway of vinylene induction in polyethylene by bacteria is still unclear (Peixoto et al., 2017); but decarboxylation of fatty acids and polyketide synthase pathway can produce alkenes (Kang and Nielsen, 2017).

Carbonyl (C=O) formation is commonly taken as an indication of LDPE oxidation (Yang et al., 2014). Absorption bands at 1,715–1,740 cm^{-1} signifies ester and keto carbonyl peaks. As previously stated, *B. siamensis* reportedly have laccase activity, and laccase may have an important role in oxidation of the hydrocarbon spine of polyethylene (Santo et al., 2013).

The FT-ICR MS analysis confirmed that many metabolites were generated in the treated sample. A total of 1448 newly generated peaks were identified in the positive ion mode, including 238 CHO and 1210 CHON chemical species. A total of 386 newly generated chemical species were identified in the negative mode, including 198 CHO and 188 CHON species. The van Krevelen diagram of the chemical species identified in both positive and negative modes were constructed (Fig. S13, Supplementary Material). From the van Krevelen diagram analysis for CHO compounds (Fig. 4b), we also observed the compositional shift of the detected compounds in the treated sample compared to the control (i.e., LDPE incubated without bacteria). The downward H/C compositional shift of the compounds indicates an increase in the degree of unsaturation of the components, in keeping with alkene group formation evidenced in FTIR spectrum. The rightward O/C compositional shift indicates an increment in the oxygen-to-carbon ratio, which is presumably related to higher oxidation states. These compositional changes were consistent in both positive and negative modes.

The van Krevelen diagram for suspected metabolite types was reconstructed from earlier studies (Bianco et al., 2018; Brockman et al., 2018; Mann et al., 2015; Wozniak et al., 2008) and superimposed on our data. Fig. 4c depicts metabolites or transformed products composed of CHO and CHON found in treated samples in the positive ion mode. The detected types of transformed products are consistent with those observed in the FTIR spectrum, including lipid-like substances (molecules related to bacterial activity; i.e., fatty acids, sterols, glycerides etc.), dicarboxylic acids, aliphatic, and peptide-like (protein derived) compounds. A fascinating point to note in the diagram is that the compounds are most densely populated in the region of unsaturated hydrocarbons. This study interestingly hinted the presence of terpenoids and polyketides for the first time in any plastic biodegradation by-product (i.e., secondary metabolite) (Data S5, Supplementary Material), which can result from the presence of active methylerythritol phosphate (found in *B. subtilis*) (Julsing et al., 2007) and polyketide synthase (PKS) pathways along the usual TCA cycle. Terpenoids and polyketides are both structurally and functionally diverse families of natural products that are rich sources of pharmaceutical, industrial, and agrochemical compounds. This finding suggests future studies on the potential of terpenoid and polyketide production as plastic biodegradation by-products. Interestingly, genes associated with terpenoid and

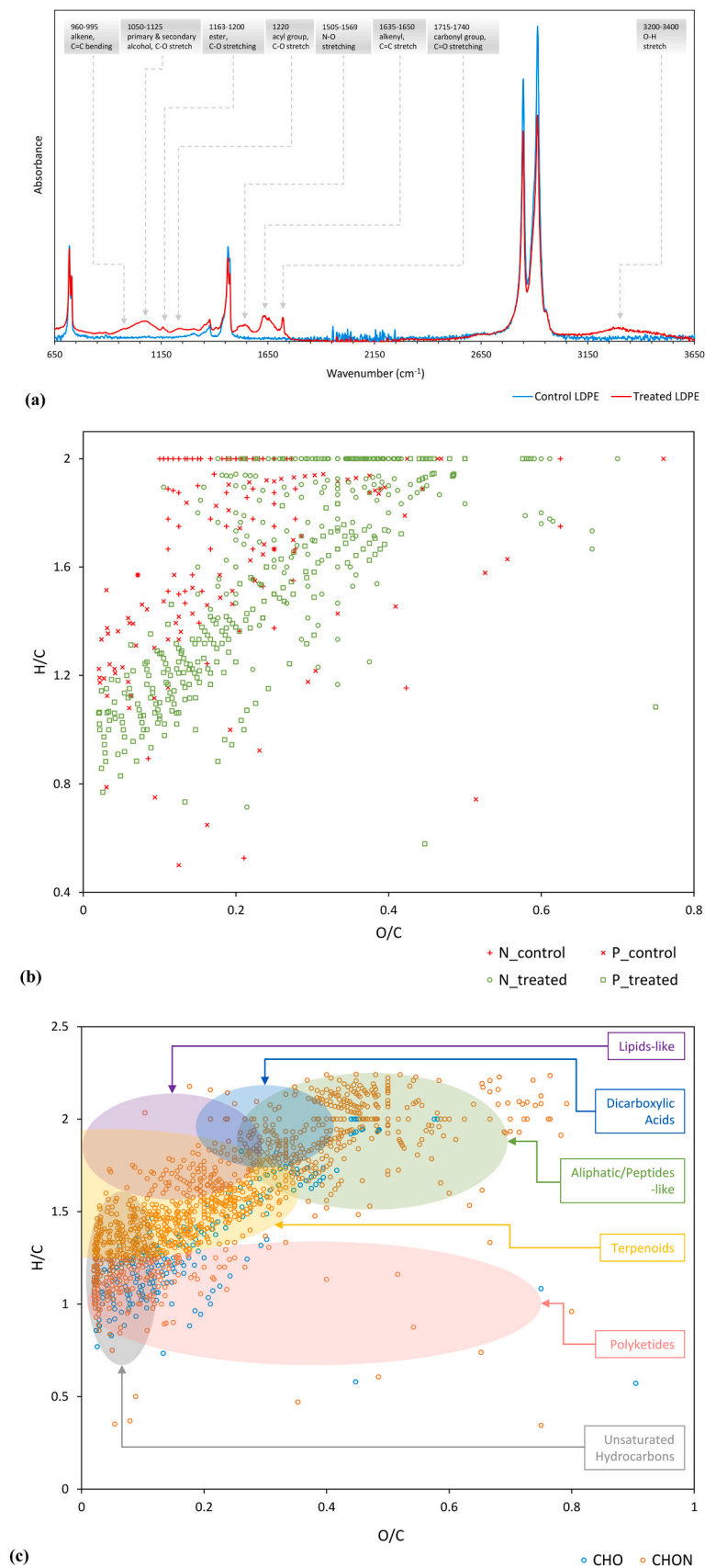


Fig. 4. (a) FTIR spectra of LDPE powder incubated (45 days) with *Bacillus siamensis* AT.KU.1 along with the control (incubated without bacteria). Newly generated peaks in the treated LDPE are indicated. (b) van Krevelen diagram of the control and treated media sample for CHO (carbon-hydrogen-oxygen) compounds in both the positive [P] and negative [N] mode. (c) van Krevelen plot for transformed products from the treated media sample: CHO and CHON (carbon-hydrogen-oxygen-nitrogen) compounds in positive mode, with probable class identifications from previous studies (Bianco et al., 2018; Brockman et al., 2018; Mann et al., 2015; Wozniak et al., 2008).

polyketide metabolism have been previously found in an indigenous strain *B. siamensis* JFL15 (Xu et al., 2018). PKS protein has been found in *Bacillus* sp. GZB (99% similar genome sequence with *B. siamensis* KCTC13613^T) (Das et al., 2019), and two PKS genes had been identified in *B. siamensis* KCTC 13613^T (Jeong et al., 2012). The successful production of secondary metabolites like polyketides and terpenoids supports the conclusion that *Bacillus siamensis* ATKU1 can use pristine LDPE as its sole carbon source.

Marine plastic debris allegedly acts as a matrix (Jacquin et al., 2019) for pathogens, pathogen dispersal by waste plastic has been studied (Silva et al., 2019), and selective endorsement of pathogenic bacterial host by microplastic biofilms has been reported (Wu et al., 2019). Many plastic degrading genera (including *Bacillus*) consist of several pathogens (Puglisi et al., 2019). In this scenario, plastic degrading, as-well-as pathogen combating ability of *Bacillus siamensis* ATKU1 make it suitable for application in large scale plastic bioremediation sites.

4. Conclusion

This is the first report on the detailed three-dimensional morphology of the developmental stages of biofilms on microplastic surfaces. This supports that indigenous bacterial species utilize microplastics as the sole carbon source. Although biofilm development was observed using a single strain in this study, this phenomenon should be very common in natural and engineered environments. For example, microplastics are frequently found in municipal wastewater treatment plants (WWTPs) applying biological treatment processes (Lee and Kim, 2018; Park et al., 2020). High LDPE removal in WWTPs is very likely to be related with biofilm development, increasing the density of microplastic particles and making them easier to sediment in WWTPs. Thus, understanding biofilm development on microplastics will help us to evaluate the fate of microplastic particles in natural and engineered environments.

Further studies on LDPE biochemical transformation pathways yielding meta-stable low molecular weight metabolites including terpenoids and polyketides are also needed to better understand environmental break-down of microplastics in aerobic environments. To examine the impact of PE molecular weight on biofilm formation and LDPE degradation, biodegradation of commercially available higher molecular weight LDPEs (M_w 20,000–90,000 Da) can be a potential future experimentation. Biofilm development on microplastic surfaces should depend on chemical properties of microplastic particles as well as environmental characteristics like redox and pH conditions. Since microplastic contamination is found to be ubiquitous (Michels et al., 2018), it is worth investigating different strains with effect on different plastic materials in the presence or absence of common plastic additives like plasticizers, antioxidants, and flame retardants.

The isolated LDPE-degrading bacteria *B. siamensis*, previously found in Thai salted food (Sumpavapol et al., 2010), has already been shown to have some beneficiary effects. Studies found that it has positive environmental impacts like plant growth endorsement via volatile emissions and generation of antimicrobial compounds (Jeong et al., 2012). More endeavors in research on the biodegradation capabilities of this indigenous strain can motivate a practical perspective to deal with the issues related to industrial plastic waste and the “new-age” microplastic problem.

CRediT authorship contribution statement

Ahrajyoti Tarafdar: Conceptualization, Data curation, Investigation, Methodology, Writing - original draft. **Jae-Ung Lee:** Investigation, Methodology, Writing - original draft. **Ji-Eun Jeong:** Investigation. **Hanbyul Lee:** Investigation, Methodology, Writing - original draft. **Yerin Jung:** Data curation. **Han Bin Oh:** Conceptualization, Writing - review & editing. **Han Young Woo:** Investigation. **Jung-Hwan Kwon:** Conceptualization, Supervision, Funding acquisition, Writing - review & editing.

Supplementary material

Physical and chemical properties of the polyethylene used; Roughness parameters used in AFM study; Microscopic particle size analysis of the LDPE used in the study; Characterization of soil properties, clay-sand-silt analysis of the collected soil sample; The microscopic particle size characterization of the collected soil; Phylogenetic tree of representative 16S rRNA gene sequences; SEM picture of the strain ATKU1; Light microscopic images of pristine and treated LDPE particles with developed biofilms on the surface of the treated particles; SEM image of the control LDPE surface; Marked area in the figure where it looked smoother and typical textures of LDPE were removed; Roughness parameters of the evolving biofilm; Pictorial depiction of surface topographies for Skewness and Kurtosis maps; Young's modulus of the LDPE surface significantly increased after the 45-day treatment; Live/Dead cell imaging for final day of control (media without carbon source/LDPE); van Krevelen plot for transformed products (CHO and CHON compounds) from the treated media sample (positive and negative mode); Mass reduction study of LDPE; Definition of Young's modulus and its interpretation in AFM study; DSC (Differential Scanning Calorimeter) analysis of LDPE; GPC (Gel Permeation Chromatography) of treated LDPE; Elemental compositions observed in the FT-ICR mass spectra that can be assigned to terpenoids and polyketides.

Declaration of Competing Interest

The authors declare that they have no known competing financial interests or personal relationships that could have appeared to influence the work reported in this paper.

Acknowledgments

This study was supported by the National Research Foundation of Korea (NRF) grant funded by the Korea government (MEST) (no. 2020R1A2C2009244). H.Y.W. is grateful for the financial support from the National Research Foundation (NRF) of Korea (NRF-2019R1A6A1A11044070). Authors are thankful to Ms. Yeonjae Yoo, Division of Environmental Science and Ecological Engineering, Korea University, for her valuable suggestions regarding phylogenetic tree construction. The authors also thank Editage (www.editage.co.kr) for providing language editing guidance and Park Systems for their kind instrumental assistance.

Conflict of interest

Authors declare no conflicting interests.

Appendix A. Supporting information

Supplementary data associated with this article can be found in the online version at [doi:10.1016/j.jhazmat.2020.124516](https://doi.org/10.1016/j.jhazmat.2020.124516).

References

- Al-Salem, S.M., 2019. Influential parameters on natural weathering under harsh climatic conditions of mechanically recycled plastic film specimens. *J. Environ. Manag.* 230, 355–365. <https://doi.org/10.1016/j.jenvman.2018.09.044>.
- Al-Salem, S.M., Abraham, G., Al-Qabandi, O.A., Dashti, A.M., 2015. Investigating the effect of accelerated weathering on the mechanical and physical properties of high content plastic solid waste (PSW) blends with virgin linear low density polyethylene (LLDPE). *Polym. Test.* 46, 116–121. <https://doi.org/10.1016/j.polymertesting.2015.07.008>.
- Albertsson, A.C., Andersson, S.O., Karlsson, S., 1987. The mechanism of biodegradation of polyethylene. *Polym. Degrad. Stab.* 18, 73–87. [https://doi.org/10.1016/0141-3910\(87\)90084-X](https://doi.org/10.1016/0141-3910(87)90084-X).
- Arora, D.P., Hossain, S., Xu, Y., Boon, E.M., 2015. Nitric oxide regulation of bacterial biofilms. *Biochemistry* 54, 3717–3728. <https://doi.org/10.1021/bi501476n>.
- Baptista Neto, J.A., Gaylarde, C., Beech, I., Bastos, A.C., da Silva Quaresma, V., de Carvalho, D.G., 2019. Microplastics and attached microorganisms in sediments of

- the Vitória bay estuarine system in SE Brazil. *Ocean Coast. Manag* 169, 247–253. <https://doi.org/10.1016/j.ocecoaman.2018.12.030>.
- Basto, M.N., Nicastró, K.R., Tavares, A.I., McQuaid, C.D., Casero, M., Azevedo, F., Zardi, G.I., 2019. Plastic ingestion in aquatic birds in Portugal. *Mar. Pollut. Bull.* 138, 19–24. <https://doi.org/10.1016/j.marpolbul.2018.11.024>.
- Begum, M.S., Jang, I., Lee, J.M., Oh, H., Bin, Jin, H., Park, J.H., 2019. Synergistic effects of urban tributary mixing on dissolved organic matter biodegradation in an impounded river system. *Sci. Total Environ.* 676, 105–119. <https://doi.org/10.1016/j.scitotenv.2019.04.123>.
- Benítez, A., Sánchez, J.J., Arnal, M.L., Müller, A.J., Rodríguez, O., 2013. Abiotic degradation of LDPE and LLDPE formulated with a pro-oxidant additive. *Polym. Degrad. Stab.* 98, 490–501. <https://doi.org/10.1016/j.polydegradstab.2012.12.011>.
- Bianco, A., Deguillaume, L., Vaïtilingom, M., Nicol, E., Baray, J.L., Chaumerliac, N., Bridoux, M., 2018. Molecular characterization of cloud water samples collected at the Puy de Dôme (France) by Fourier transform ion cyclotron resonance mass spectrometry. *Environ. Sci. Technol.* 52, 10275–10285. <https://doi.org/10.1021/acs.est.8b01964>.
- Botterell, Z.L.R., Beaumont, N., Dorrington, T., Steinke, M., Thompson, R.C., Lindeque, P. K., 2019. Bioavailability and effects of microplastics on marine zooplankton: a review. *Environ. Pollut.* 245, 98–110. <https://doi.org/10.1016/j.envpol.2018.10.065>.
- Brockman, S.A., Roden, E.V., Hegeman, A.D., 2018. Van Krevelen diagram visualization of high resolution-mass spectrometry metabolomics data with OpenVanKrevelen. *Metabolomics* 14, 1–5. <https://doi.org/10.1007/s11306-018-1343-y>.
- Campani, T., Bainsi, M., Giannetti, M., Cancelli, F., Mancusi, C., Serena, F., Marsili, L., Casini, S., Fossi, M.C., 2013. Presence of plastic debris in loggerhead turtle stranded along the Tuscan coasts of the Pelagos Sanctuary for Mediterranean Marine Mammals (Italy). *Mar. Pollut. Bull.* 74, 225–230. <https://doi.org/10.1016/j.marpolbul.2013.06.053>.
- Chatterjee, S., Biswas, N., Datta, A., Dey, R., Maiti, P., 2014. Atomic force microscopy in biofilm study. *Microscopy* 63, 269–278. <https://doi.org/10.1093/jmicro/dfu013>.
- Chauhan, D., Agrawal, G., Deshmukh, S., Roy, S.S., Priyadarshini, R., 2018. Biofilm formation by *Exiguobacterium* sp. DR11 and DR14 alter polystyrene surface properties and initiate biodegradation. *RSC Adv.* 8, 37590–37599. <https://doi.org/10.1039/C8RA06448B>.
- Das, R., Liang, Z., Li, G., Mai, B., An, T., 2019. Genome sequence of a spore-laccase forming, BPA-degrading *Bacillus* sp. GZB isolated from an electronic-waste recycling site reveals insights into BPA degradation pathways. *Arch. Microbiol.* 201, 623–638. <https://doi.org/10.1007/s00203-019-01622-2>.
- Erni-Cassola, G., Zadjelovic, V., Gibson, M.I., Christie-Oleza, J.A., 2019. Distribution of plastic polymer types in the marine environment; a meta-analysis. *J. Hazard. Mater.* 369, 691–698. <https://doi.org/10.1016/j.jhazmat.2019.02.067>.
- Eyheraguibel, B., Traikia, M., Fontanella, S., Sancelme, M., Bonhomme, S., Fromageot, D., Lemaire, J., Lauranson, G., Lacoste, J., Delort, A.M., 2017. Characterization of oxidized oligomers from polyethylene films by mass spectrometry and NMR spectroscopy before and after biodegradation by a *Rhodococcus rhodochrous* strain. *Chemosphere* 184, 366–374. <https://doi.org/10.1016/j.chemosphere.2017.05.137>.
- Fan, B., Blom, J., Klenk, H.P., Borriss, R., 2017. *Bacillus amyloliquefaciens*, *Bacillus velezensis*, and *Bacillus siamensis* form an “Operational Group *B. amyloliquefaciens*” within the *B. subtilis* species complex. *Front. Microbiol.* 8, 1–15. <https://doi.org/10.3389/fmicb.2017.00022>.
- Garside, M., 2019. Global plastic production [WWW Document]. Statista. URL (<https://www.statista.com/statistics/282732/global-production-of-plastics-since-1950/>) (Accessed 11.15.19).
- Gong, G., Kim, S., Lee, S.M., Woo, H.M., Park, T.H., Um, Y., 2017. Complete genome sequence of *Bacillus* sp. 275, producing extracellular cellulolytic, xylanolytic and ligninolytic enzymes. *J. Biotechnol.* 254, 59–62. <https://doi.org/10.1016/j.jbiotec.2017.05.021>.
- Harrison, J.P., Schratzberger, M., Sapp, M., Osborn, A.M., 2014. Rapid bacterial colonization of low-density polyethylene microplastics in coastal sediment microcosms. *BMC Microbiol.* 14, 1–15. <https://doi.org/10.1186/s12866-014-0232-4>.
- Harshvardhan, K., Jha, B., 2013. Biodegradation of low-density polyethylene by marine bacteria from pelagic waters, Arabian Sea, India. *Mar. Pollut. Bull.* 77, 100–106. <https://doi.org/10.1016/j.marpolbul.2013.10.025>.
- Hernandez-Gonzalez, A., Saavedra, C., Gago, J., Covelo, P., Santos, M.B., Pierce, G.J., 2018. Microplastics in the stomach contents of common dolphin (*Delphinus delphis*) stranded on the Galician coasts (NW Spain, 2005–2010). *Mar. Pollut. Bull.* 137, 526–532. <https://doi.org/10.1016/j.marpolbul.2018.10.026>.
- Holden, J.K., Dejam, D., Lewis, M.C., Huang, H., Kang, S., Jing, Q., Xue, F., Silverman, R. B., Poulos, T.L., 2015. Inhibitor bound crystal structures of bacterial nitric oxide synthase. *Biochemistry* 54, 4075–4082. <https://doi.org/10.1021/acs.biochem.5b00431>.
- Hossain, S., Nisbett, L.M., Boon, E.M., 2017. Discovery of two bacterial nitric oxide-responsive proteins and their roles in bacterial biofilm regulation. *Acc. Chem. Res.* 50, 1633–1639. <https://doi.org/10.1021/acs.accounts.7b00095>.
- Huang, Q., Wu, H., Cai, P., Fein, J.B., Chen, W., 2015. Atomic force microscopy measurements of bacterial adhesion and biofilm formation onto clay-sized particles. *Sci. Rep.* 5, 1–12. <https://doi.org/10.1038/srep16857>.
- Jacquin, J., Cheng, J., Odobel, C., Pandin, C., Conan, P., Pujo-Pay, M., Barbe, V., Meistertzheim, A.L., Ghiglione, J.F., 2019. Microbial ecotoxicology of marine plastic debris: a review on colonization and biodegradation by the “Plastisphere”. *Front. Microbiol.* 10, 1–16. <https://doi.org/10.3389/fmicb.2019.00865>.
- Jeong, H., Jeong, D.E., Kim, S.H., Song, G.C., Park, S.Y., Ryu, C.M., Park, S.H., Choi, S.K., 2012. Draft genome sequence of the plant growth-promoting bacterium *Bacillus siamensis* KCTC 13613T. *J. Bacteriol.* 194, 4148–4149. <https://doi.org/10.1128/JB.00805-12>.
- Jiang, P., Zhao, S., Zhu, L., Li, D., 2018. Microplastic-associated bacterial assemblages in the intertidal zone of the Yangtze Estuary. *Sci. Total Environ.* 624, 48–54. <https://doi.org/10.1016/j.scitotenv.2017.12.105>.
- John, C., 2000. Interpretation of infrared spectra, a practical approach. *Encycl. Anal. Chem.* 10815–10837.
- Julsing, M.K., Rijpkema, M., Woerdenbag, H.J., Quax, W.J., Kayser, O., 2007. Functional analysis of genes involved in the biosynthesis of isoprene in *Bacillus subtilis*. *Appl. Microbiol. Biotechnol.* 75, 1377–1384. <https://doi.org/10.1007/s00253-007-0953-5>.
- Jung, M.R., Horgen, F.D., Orski, S.V., Rodriguez, C., V., Beers, K.L., Balazs, G.H., Jones, T.T., Work, T.M., Brignac, K.C., Royer, S.J., Hyrenbach, K.D., Jensen, B.A., Lynch, J.M., 2018. Validation of ATR FT-IR to identify polymers of plastic marine debris, including those ingested by marine organisms. *Mar. Pollut. Bull.* 127, 704–716. <https://doi.org/10.1016/j.marpolbul.2017.12.061>.
- Kang, M.K., Nielsen, J., 2017. Biobased production of alkanes and alkenes through metabolic engineering of microorganisms. *J. Ind. Microbiol. Biotechnol.* 44, 613–622. <https://doi.org/10.1007/s10295-016-1814-y>.
- Kim, S., Kramer, R.W., Hatcher, P.G., 2003. Graphical method for analysis of ultrahigh-resolution broadband mass spectra of natural organic matter, the van Krevelen Diagram. *Anal. Chem.* 75, 5336–5344. <https://doi.org/10.1021/ac034415p>.
- Kirstein, I.V., Wichels, A., Krohne, G., Gerds, G., 2018. Mature biofilm communities on synthetic polymers in seawater - specific or general? *Mar. Environ. Res.* 142, 147–154. <https://doi.org/10.1016/j.marenvres.2018.09.028>.
- Van Krevelen, D.W., 1950. Graphical statistical method for the study of structure and reaction processes of coal. *Fuel* 29, 269–284.
- Lee, H., Kim, Y., 2018. Treatment characteristics of microplastics at biological sewage treatment facilities in Korea. *Mar. Pollut. Bull.* 137, 1–8. <https://doi.org/10.1016/j.marpolbul.2018.09.050>.
- Liu, L., Li, X., Nonaka, K., 2015. Light depolarization in off-specular reflection on submicron rough metal surfaces with imperfectly random roughness. *Rev. Sci. Instrum.* 86. <https://doi.org/10.1063/1.4908172>.
- Lusher, A.L., Hernandez-Milian, G., Berrow, S., Rogan, E., O’Connor, I., 2018. Incidence of marine debris in cetaceans stranded and bycaught in Ireland: recent findings and a review of historical knowledge. *Environ. Pollut.* 232, 467–476. <https://doi.org/10.1016/j.envpol.2017.09.070>.
- Mann, B.F., Chen, H., Herndon, E.M., Chu, R.K., Tolic, N., Portier, E.F., Chowdhury, T.R., Robinson, E.W., Callister, S.J., Wullschlegel, S.D., Graham, D.E., Liang, L., Gu, B., 2015. Indexing permafrost soil organic matter degradation using high-resolution mass spectrometry. *PLoS One* 10, 1–16. <https://doi.org/10.1371/journal.pone.0130557>.
- Mathieu-Denoncourt, J., Wallace, S.J., de Solla, S.R., Langlois, V.S., 2015. Plasticizer endocrine disruption: highlighting developmental and reproductive effects in mammals and non-mammalian aquatic species. *Gen. Comp. Endocrinol.* 219, 74–88. <https://doi.org/10.1016/j.ygcen.2014.11.003>.
- Miao, L., Wang, P., Hou, J., Yao, Y., Liu, Z., Liu, S., Li, T., 2019. Distinct community structure and microbial functions of biofilms colonizing microplastics. *Sci. Total Environ.* 650, 2395–2402. <https://doi.org/10.1016/j.scitotenv.2018.09.378>.
- Michels, J., Stippkugel, A., Lenz, M., Wirtz, K., Engel, A., 2018. Rapid aggregation of biofilm-covered microplastics with marine biogenic particles. *Proc. R. Soc. B Biol. Sci.* 285, 20181203. <https://doi.org/10.1098/rspb.2018.1203>.
- Mukherjee, S., RoyChaudhuri, U., Kundu, P.P., 2018. Biodegradation of polyethylene via complete solubilization by the action of *Pseudomonas fluorescens*, biosurfactant produced by *Bacillus licheniformis* and anionic surfactant. *J. Chem. Technol. Biotechnol.* 93, 1300–1311. <https://doi.org/10.1002/jctb.5489>.
- Ogonowski, M., Motiej, A., Iminbergs, K., Hell, E., Gerdes, Z., Udekwu, K.I., Bacsik, Z., Gorokhova, E., 2018. Evidence for selective bacterial community structuring on microplastics. *Environ. Microbiol.* 20, 2796–2808. <https://doi.org/10.1111/1462-2920.14120>.
- Ojha, N., Pradhan, N., Singh, S., Barla, A., Shrivastava, A., Khatua, P., Rai, V., Bose, S., 2017. Evaluation of HDPE and LDPE degradation by fungus, implemented by statistical optimization. *Sci. Rep.* 7, 1–13. <https://doi.org/10.1038/srep39515>.
- Oluwoye, I., Altarawneh, M., Gore, J., Bockhorn, H., Dlugogorski, B.Z., 2016. Oxidation of polyethylene under corrosive NOx atmosphere. *J. Phys. Chem. C* 120, 3766–3775. <https://doi.org/10.1021/acs.jpcc.5b10466>.
- Paço, A., Duarte, K., da Costa, J.P., Santos, P.S.M., Pereira, R., Pereira, M.E., Freitas, A.C., Duarte, A.C., Rocha-Santos, T.A.P., 2017. Biodegradation of polyethylene microplastics by the marine fungus *Zalerion maritimum*. *Sci. Total Environ.* 586, 10–15. <https://doi.org/10.1016/j.scitotenv.2017.02.017>.
- Pan, H.-Q., Ju, J.-H., 2018. Genome sequence and genome mining of multiple bioactive secondary metabolites from a deep sea-derived *Bacillus siamensis* SC510 05746. [WWW Document]. URL (<https://www.uniprot.org/uniprot/A0A2K9KF7>) (Accessed 11.13.19).
- Park, H., Oh, M., Kim, P., Kim, G., Jeong, D., Ju, B., Lee, W., Chung, H., Kang, H., Kwon, J., 2020. National reconnaissance survey of microplastics in municipal wastewater treatment plants in Korea. *Environ. Sci. Technol.* 54, 1503–1512. <https://doi.org/10.1021/acs.est.9b04929>.
- Parrish, K., Fahrenfeld, N.L., 2019. Microplastic biofilm in fresh- and wastewater as a function of microparticle type and size class. *Environ. Sci. Water Res. Technol.* 5, 495–505. <https://doi.org/10.1039/c8ew00712h>.
- Parthipan, P., Preetham, E., Machuca, L.L., Rahman, P.K.S.M., Murugan, K., Rajasekar, A., 2017. Biosurfactant and degradative enzymes mediated crude oil

- degradation by bacterium *Bacillus subtilis* A1. *Front. Microbiol* 8, 1–14. <https://doi.org/10.3389/fmicb.2017.00193>.
- Peixoto, J., Silva, L.P., Krüger, R.H., 2017. Brazilian Cerrado soil reveals an untapped microbial potential for unpretreated polyethylene biodegradation. *J. Hazard. Mater.* 324, 634–644. <https://doi.org/10.1016/j.jhazmat.2016.11.037>.
- Pinto, M., Langer, T.M., Hüffer, T., Hofmann, T., Herndl, G.J., 2019. The composition of bacterial communities associated with plastic biofilms differs between different polymers and stages of biofilm succession. *PLoS One* 14, 1–20. <https://doi.org/10.1371/journal.pone.0217165>.
- Pinto, C., Sousa, S., Froufe, H., Egas, C., Clément, C., Fontaine, F., Gomes, A.C., 2018. Draft genome sequence of *Bacillus amyloliquefaciens* subsp. plantarum strain Fito-F321, an endophyte microorganism from *Vitis vinifera* with biocontrol potential. *Stand. Genom. Sci.* 13, 1–12. <https://doi.org/10.1186/s40793-018-0327-x>.
- Plastics Europe & EPRO, 2016. *Plastics – the Facts 2016*, *Plastics – the Facts 2016*. (<http://doi.org/10.1016/j.marpolbul.2013.01.015>).
- Puglisi, E., Romaniello, F., Galletti, S., Boccaleri, E., Frache, A., Cocconcelli, P.S., 2019. Selective bacterial colonization processes on polyethylene waste samples in an abandoned landfill site. *Sci. Rep.* 9, 1–13. <https://doi.org/10.1038/s41598-019-50740-w>.
- Rummel, C.D., Jahnke, A., Gorokhova, E., Kühnel, D., Schmitt-Jansen, M., 2017. Impacts of biofilm formation on the fate and potential effects of microplastic in the aquatic environment. *Environ. Sci. Technol. Lett.* 4, 258–267. <https://doi.org/10.1021/acs.estlett.7b00164>.
- Dos Santos, A.L.S., Galdino, A.C.M., de Mello, T.P., Ramos, L., de, S., Branquinha, M.H., Bolognese, A.M., Neto, J.C., Roudbary, M., 2018. What are the advantages of living in a community? A microbial biofilm perspective! *Mem. Inst. Oswaldo Cruz* 113, 1–7. <https://doi.org/10.1590/0074-02760180212>.
- Santo, M., Weitsman, R., Sivan, A., 2013. The role of the copper-binding enzyme - laccase - in the biodegradation of polyethylene by the actinomycete *Rhodococcus ruber*. *Int. Biodeterior. Biodegrad.* 84, 204–210. <https://doi.org/10.1016/j.ibiod.2012.03.001>.
- Sathish, N., Jeyasanta, K.I., Patterson, J., 2019. Abundance, characteristics and surface degradation features of microplastics in beach sediments of five coastal areas in Tamil Nadu, India. *Mar. Pollut. Bull.* 142, 112–118. <https://doi.org/10.1016/j.marpolbul.2019.03.037>.
- Silva, M.M., Maldonado, G.C., Castro, R.O., de Sá Felizardo, J., Cardoso, R.P., Anjos, R.M., dos, Araújo, F.V. de, 2019. Dispersal of potentially pathogenic bacteria by plastic debris in Guanabara Bay, RJ, Brazil. *Mar. Pollut. Bull.* 141, 561–568. <https://doi.org/10.1016/j.marpolbul.2019.02.064>.
- Sivan, A., Szanto, M., Pavlov, V., 2006. Biofilm development of the polyethylene-degrading bacterium *Rhodococcus ruber*. *Appl. Microbiol. Biotechnol.* 72, 346–352. <https://doi.org/10.1007/s00253-005-0259-4>.
- Stelfox, M., Hudgins, J., Sweet, M., 2016. A review of ghost gear entanglement amongst marine mammals, reptiles and elasmobranchs. *Mar. Pollut. Bull.* 111, 6–17. <https://doi.org/10.1016/j.marpolbul.2016.06.034>.
- Sumpavapol, P., Tongyong, L., Tanasupawat, S., Chokesajjawatee, N., Luxananil, P., Visessanguan, W., 2010. *Bacillus siamensis* sp. nov., isolated from salted crab (pookhem) in Thailand. *Int. J. Syst. Evol. Microbiol.* 60, 2364–2370. <https://doi.org/10.1099/ijss.0.018879-0>.
- Tarafdar, A., Sarkar, T.K., Chakraborty, S., Sinha, A., Mastro, R.E., 2018. Biofilm development of *Bacillus thuringiensis* on MWCNT buckypaper: adsorption-synergic biodegradation of phenanthrene. *Ecotoxicol. Environ. Saf.* 157, 327–334. <https://doi.org/10.1016/j.ecoenv.2018.03.090>.
- Tarafdar, A., Sinha, A., Mastro, R.E., 2017. Biodegradation of anthracene by a newly isolated bacterial strain, *Bacillus thuringiensis* AT. ISM.1, isolated from a fly ash deposition site. *Lett. Appl. Microbiol.* 65, 327–334. <https://doi.org/10.1111/lam.12785>.
- Tavares, A.C., Gulmine, J. V., Lepienski, C.M., Akcelrud, L., 2003. The effect of accelerated aging on the surface mechanical properties of polyethylene 81, 367–373. ([https://doi.org/10.1016/S0141-3910\(03\)00108-3](https://doi.org/10.1016/S0141-3910(03)00108-3)).
- United Nations, 2018. *The state of plastics: World Environment Day Outlook 2018*. UN Environ. Program. 11. (<https://doi.org/10.1093/oxfordhb/9780199238804.003.0031>).
- Wang, W., Yu, X., 2020. Bioavailability and toxicity of microplastics to fish species: a review. *Ecotoxicol. Environ. Saf.* 189, 109913. <https://doi.org/10.1016/j.ecoenv.2019.109913>.
- Wozniak, A.S., Bauer, J.E.T., Sleighter, R.L., Dickhut, R.M., Hatcher, P.G., 2008. Technical note: molecular characterization of aerosol-derived water soluble organic carbon using ultrahigh resolution electrospray ionization Fourier transform ion cyclotron resonance mass spectrometry. *Atmos. Chem. Phys.* 8, 5099–5111. <https://doi.org/10.5194/acp-8-5099-2008>.
- Wu, X., Pan, J., Li, M., Li, Y., Bartlam, M., Wang, Y., 2019. Selective enrichment of bacterial pathogens by microplastic biofilm. *Water Res.* 165, 114979. <https://doi.org/10.1016/j.watres.2019.114979>.
- Xu, B.H., Lu, Y.Q., Ye, Z.W., Zheng, Q.W., Wei, T., Lin, J.F., Guo, L.Q., 2018. Genomics-guided discovery and structure identification of cyclic lipopeptides from the *Bacillus siamensis* JFL15. *PLoS One* 13, 1–18. <https://doi.org/10.1371/journal.pone.0202893>.
- Yang, J., Yang, Y., Wu, W.M., Zhao, J., Jiang, L., 2014. Evidence of polyethylene biodegradation by bacterial strains from the guts of plastic-eating waxworms. *Environ. Sci. Technol.* 48, 13776–13784. <https://doi.org/10.1021/es504038a>.
- Yoon, S.H., Ha, S.M., Kwon, S., Lim, J., Kim, Y., Seo, H., Chun, J., 2017. Introducing EzBioCloud: a taxonomically united database of 16S rRNA gene sequences and whole-genome assemblies. *Int. J. Syst. Evol. Microbiol.* 67, 1613–1617. <https://doi.org/10.1099/ijsem.0.001755>.
- Yoo, Y., Lee, D.W., Lee, H., Kwon, B.O., Khim, J.S., Yim, U.H., Park, H., Park, B., Choi, I. G., Kim, B.S., Jeon, S.W., Kim, G.H., Kim, J.J., 2019. *Gemmobacter lutimaris* sp. nov., a marine bacterium isolated from a tidal flat. *Int. J. Syst. Evol. Microbiol.* 69, 1676–1681. <https://doi.org/10.1099/ijsem.0.003375>.
- Zettler, E.R., Mincer, T.J., Amaral-Zettler, L.A., 2013. Life in the “plastisphere”: microbial communities on plastic marine debris. *Environ. Sci. Technol.* 47, 7137–7146. <https://doi.org/10.1021/es401288x>.